

Design and Computational Fluid Dynamics Analysis of an Idealized Modern Wingsuit

Maria E. Ferguson
Washington University in St. Louis
Advisor: Dr. Ramesh K. Agarwal

Abstract

The modern wingsuit has been the subject of few scientific studies to date; the prevailing design process remains the dangerous “guess-and-check” method. This study employed the commercial CFD flow solver ANSYS Fluent to solve the steady Reynolds Averaged Navier-Stokes equations with several turbulence models. The computational fluid dynamics (CFD) results provided information on the flow about a wingsuit designed with an airfoil cross section and relatively large planform with aspect ratio 1.3 at a Reynolds number of 5.5×10^6 . The CFD simulations were performed using the k- κ - ω Transition turbulence model for the 2D Gottingen 228 airfoil and with the Spalart-Allmaras turbulence model for the 3D wingsuit. Although the lack of experimental data available for the wingsuit flight makes the true CFD validation difficult, the results for the 3D wingsuit were analyzed and compared to the 2D airfoil, for which the computations were validated against the data from the airfoil/wing management software Profili 2.0. The Gottingen 228 airfoil had a maximum lift coefficient of 1.97 and a stall angle of 13° . The wingsuit had a maximum lift coefficient of 2.73 and reached a stall angle of 48° , which is higher than that of the 2D airfoil due to the 3D planform and induced drag. The computational results indicate that the wingsuit as designed shows promise and could likely perform well under typical wingsuit flying conditions.

Introduction

Unlike a hang glider, jet pack, or small plane, the wingsuit avoids excessive apparatus or motors and allows the flyer to glide on his/her power. It is made of flexible and durable parachute fabric that inflates while in flight. Wingsuit connects the limbs to create a wing with as much lift as possible given the limitations of the human body. The modern wingsuit has only been in existence since the 1990s [1], and although academics and manufacturers have begun to take a more scientific approach to wingsuit design, only a handful of truly rigorous analyses have been done thus far. The lack of information on wingsuit aerodynamics puts designers and flyers at a dangerous disadvantage; however the computational fluid dynamics (CFD) approaches can provide risk-free information prior to the experimental trial stage.

The first step in creating a computer simulation of a wingsuit in flight is to generate the geometry of the wingsuit. Partly due to issues of intellectual property along with the flexible nature of the wingsuit, it is difficult to generate a geometry that exactly matches a commercial wingsuit. In addition, computational limitations require that for the present, the wingsuit should be assumed rigid. The project was therefore approached in an idealized fashion: at a certain instant in time, the wingsuit has a certain shape and the rigid geometry reflects that shape at that moment. Furthermore, the ideal cross section for a wingsuit is an airfoil, although the contours of the human body and the flexible fabric make this ideal unattainable. The cross section of the wingsuit in this study was assumed to be an airfoil. The idealized scenario lent itself to a comparison of the 2D results for the chosen airfoil cross section and the 3D results for the wingsuit geometry, since the theoretical analyses already exist to compare a wing and its cross

section. Although there is no experimental data readily available for wingsuits, the airfoil/wing management software Profili 2.0 is used to generate lift and drag data, which is then used to validate the 2D airfoil case.

In 2D, the angle of attack of the air coming towards the leading edge of the airfoil is the angle of attack the airfoil experiences. In wing theory, however, the airfoil cross sections on the wing experience an induced drag caused by the downwash, a phenomenon where a small velocity component points downward toward the wing upper surface [2]. This leads to an induced angle of attack, which must be subtracted from the geometric angle of attack to obtain the effective angle of attack (the term “angle of attack” in the following text and plots shall indicate the geometric angle of attack unless mentioned otherwise). The effective angle of attack for a wing is then calculated as [2]

$$\alpha_{eff} = \alpha - \alpha_i \quad (1)$$

where α is the geometric angle of attack and α_i is the induced angle of attack. The induced angle of attack is easily calculated by approximating the wingsuit as an elliptic wing. This is a big assumption, but here the motivation is to observe a trend rather than obtain exact values, therefore it is sufficient as an approximation. The following equation from [2] is then used to determine α_i .

$$\alpha_i = \frac{C_L}{\pi AR} \quad (2)$$

When the plot of lift coefficient vs. angle of attack for a 2D airfoil is compared to that of a 3D wing, it is expected that the 3D curve will reach a higher angle of attack before stall and will have a somewhat similar slope according to the relation given in [2]:

$$\frac{dC_L}{d\alpha} = a = \frac{a_0}{1 + \frac{a_0}{\pi AR(1+\tau)}} \quad (3)$$

The value of τ varies depending upon the wing planform; $\tau = 0$ for an elliptic wing.

Geometry

Due to the flexible nature of the wingsuit, it is all but impossible to pinpoint its exact geometry in flight. The geometry was designed as an idealized approximation of the typical planform and cross section of suits currently on the market. The human body, including head, hands, feet, and body contours, was excluded from the geometry, as was the parachute pack that typically rests like a backpack over the flyer’s back.

Since the design was meant to reflect the ideal wingsuit, it was created with an airfoil cross section. The 2D airfoil section was

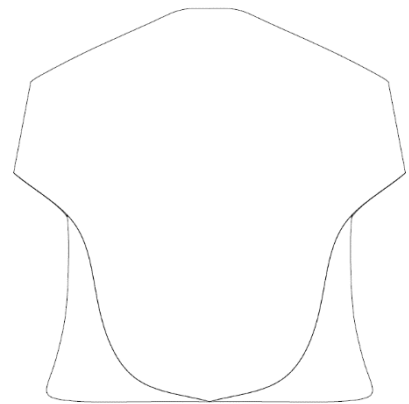


Figure 1: Wingsuit Planform

chosen for its thickness and high camber so as to have a large lift coefficient.

The 3D geometry was created with Autodesk Inventor 2016 by utilizing the “loft” feature along the line of the planform to connect a center airfoil cross section to a smaller airfoil cross section on the wing edge. The resulting wingsuit had an airfoil cross section at any section except at the very outer edges, where the airfoil cross section was parallel to the angled wing edge. The edges on the lower half of the suit, near the legs, were unrealistically thin due to the constraints of the CAD software. The thin areas are visible as the triangular portions on the lower left and right in Figure 1. The wingspan and height of the suit were designed to be 1.81 m so that the suit could accommodate the body of a tall human.

Some suits have cutouts, making a forward wing on the arms and another wing between the legs. Others stretch the fabric such that the forward wing reaches all the way to the legs as shown in Figure 1. The planform was created in imitation of the relatively larger aspect ratio suits designed for more experienced flyers. The aspect ratio of the final geometry was 1.3.

Mesh Generation in ICEM

The 2D C-mesh for the airfoil validation case was created in the ANSYS meshing software ICEM with a 25 m far field and an airfoil chord length of 1 m as shown in Figure 2. The final mesh after refinement had approximately 100,000 elements with a finer grid near the airfoil and in its wake. A more detailed view of the geometry near the airfoil is also shown in Figure 2.

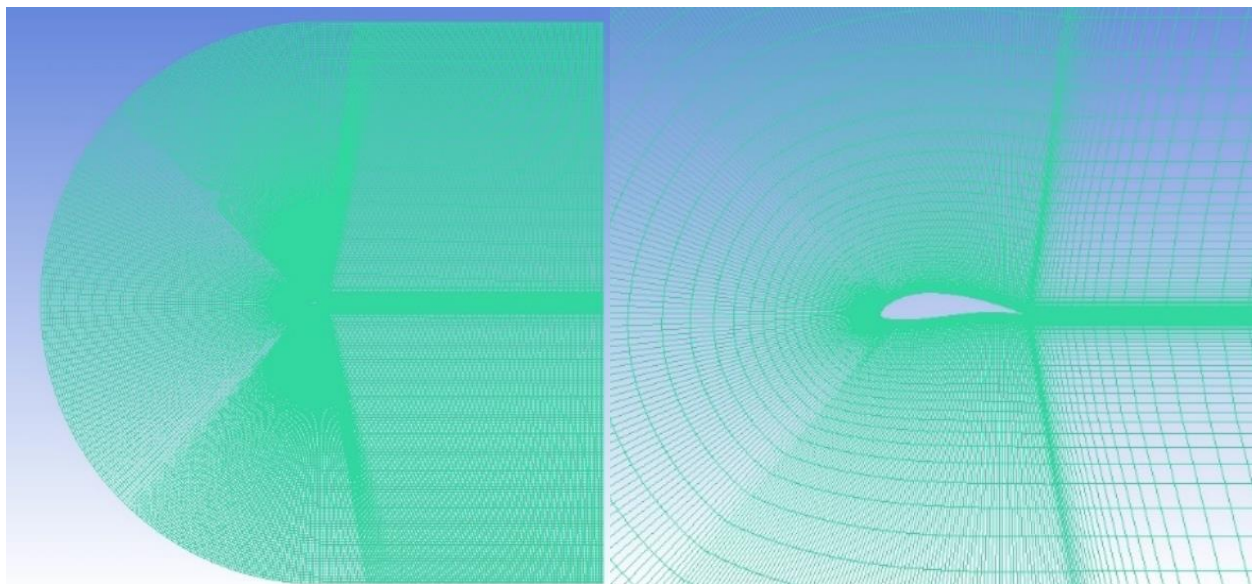


Figure 2: C-Mesh with 25 m far field (right), with detailed view near airfoil (left)

The 3D mesh was also created in ICEM and had a far field in the shape of an elliptical spheroid with major axis 60 m, minor axis 30 m, width 12 m, and a symmetry plane that cut through the middle of the wingsuit geometry. Near the wingsuit, a dense mesh region was created to achieve finer resolution closer to the geometry. The final mesh had approximately 2.4 million elements. Both meshes are shown in Figure 3.

Since there were no experimental or literature values for the wingsuit, it was of vital importance to prove the grid independence of the CFD solution that is to show that the numerical results were not dependent on the mesh and that a finer mesh would yield the same results as a relatively coarser mesh. The finer mesh was generated with the same geometry and far field, but with a smaller global element size and three dense regions with increasing mesh density towards the center. This mesh had approximately 7.4 million elements.

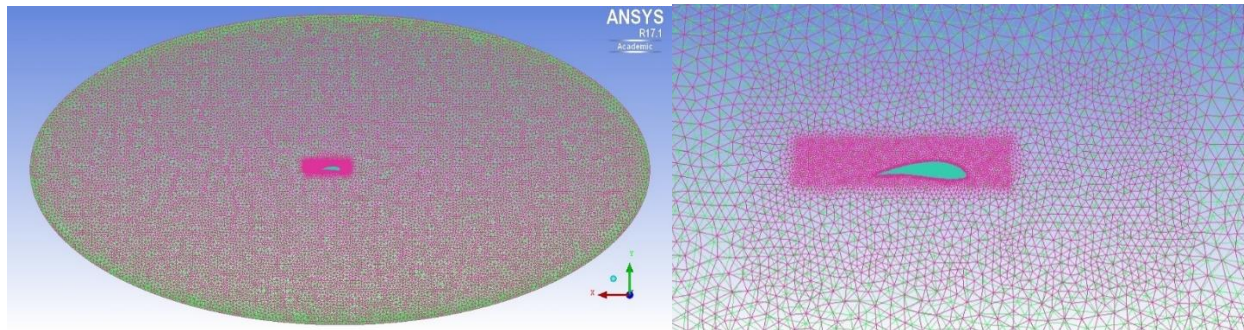


Figure 3: 2.4 million element wingsuit mesh (left) and 7.4 million element wingsuit mesh with three dense mesh regions (right)

Numerical Setup in ANSYS Fluent

The 2D airfoil case was run with a pressure-based, viscous, incompressible flow solver using the transition k-kl- ω turbulence model. The entire geometry was scaled down by a factor of 0.1 to reduce the chord length from 1 m to 0.1 m to reduce the Reynolds number to 2.4×10^5 , a value for which the computed results could be compared to values in Profili 2.0. The semi-circle in front of the leading edge of the airfoil in Figure 2 was considered a velocity inlet with a magnitude of 45 m/s, which is a reasonable value for a wingsuit flight and provides the best glide ratio at a comfortable speed [3]. The downstream boundary of the computational domain was considered a pressure outlet.

The SIMPLE solution scheme with second order upwind discretization for the momentum equations was employed. The 2D airfoil case was run for angles of attack from 0 to 14° in steps of two degrees until the lift and drag coefficients for each angle of attack converged.

The 3D wingsuit case was run with a pressure-based, viscous solver using the Spalart-Allmaras turbulence model with air density set to that of ideal gas. The plane cutting the geometry in half was set as a symmetry plane and the far field was set as a pressure far field. The free stream Mach number was set at 0.132, which corresponds to a velocity of 45 m/s. The resulting Reynolds number was approximately 3.5×10^6 . The planform area was set at 1 m^2 in order to obtain the non-dimensionalized lift and drag coefficients; these values would be later multiplied by the planform half area, 1.25 m^2 , to obtain the values for the lift and drag coefficients for the designed wingsuit. The length of the wingsuit was set at 1.84 m due to a slight measurement error (the actual length was 1.81 m). The moment coefficient was calculated about the quarter chord, at 0.46 m along the x-direction.

The SIMPLE solution scheme with second order upwind discretization for the momentum equations was also used for the 3D case. The case was run for angles of attack from 0 to 50° in

steps of two degrees until the lift and drag coefficients at each angle of attack converged within a specified tolerance of less than one percent.

Numerical Results for 2D Airfoil and 3D Wingsuit

2D Airfoil Results

The Reynolds number for the 2D airfoil case was 2.4×10^5 assuming the air properties at 10,000 ft. and a chord length of 10 cm. The software Profili 2.0 provides the airfoil data up to the angle of stall, and this data was compared to the data obtained from Fluent using the k-kl- ω model as shown in Figure 4 and Figure 5. The largest error was at 0° angle of attack, with the Fluent data 19% and 45% lower than the Profili data for lift and drag coefficient respectively. Otherwise, the data matched well and showed a maximum lift coefficient of 1.97 and stall after 12° as predicted by Profili. The success of the 2D validation case provided greater confidence for simulation of the 3D case.

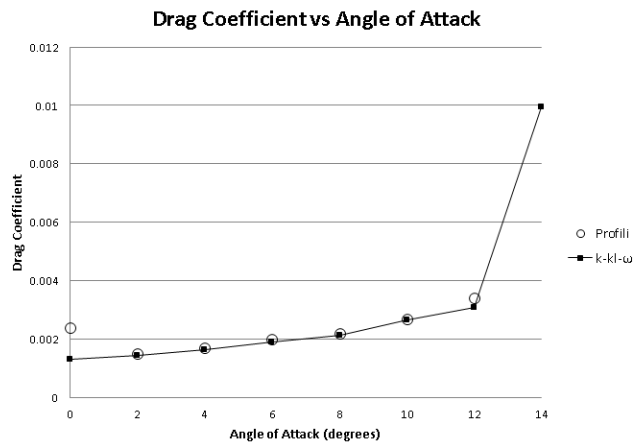


Figure 4: Drag coefficient from Profili 2.0 and Fluent

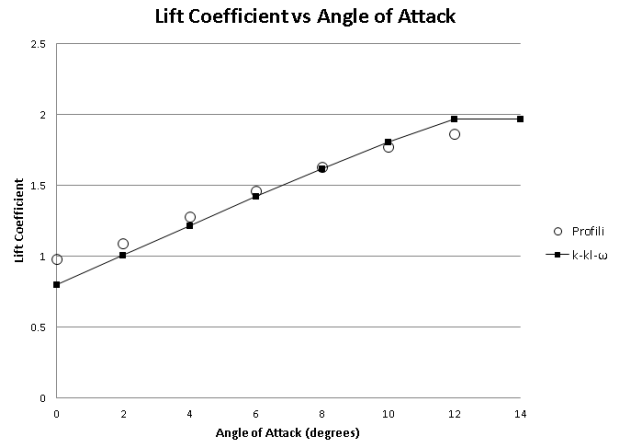


Figure 5: Lift coefficient from Profili 2.0 and Fluent

3D Wingsuit Results

The 3D cases converged within several thousand iterations until about 26° angle of attack, after which point the convergence history showed some oscillations. By 46° angle of attack, the cases were run for tens of thousands of iterations, but eventually the oscillations became small enough to consider the solution converged. The lift increased linearly until 48° angle of attack, at which point a large drop in lift became evident. Thus, 48° was considered as the stall angle for the

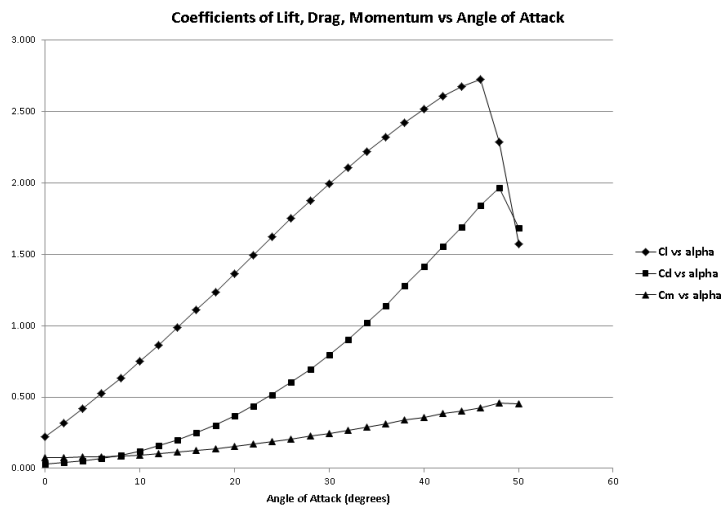


Figure 6: Coefficients of lift, drag, and moment vs. angle of attack for the wingsuit

wingsuit. The coefficients of lift, drag, and moment were multiplied by the wingsuit area to obtain the results shown in Figure 6, with a maximum lift coefficient of 2.73.

The quality of these results was evaluated in two ways: testing for mesh independence and comparing the 3D wingsuit curves to the 2D airfoil curves. The mesh independence test at 6° and 12° angles of attack produced the same results for C_D , C_L , and C_m with less than 1% error, proving that the results were independent of the mesh.

When the 3D lift curve was compared to the 2D curve, a surprisingly large value was obtained for stall close to 48° and the 3D slope of the lift curve was lower than expected from Equation (3). Based on an airfoil lift curve slope of 0.0987, the expected elliptic wing lift curve slope would give 0.0975. Although the value of τ for this unusual geometry is unknown, τ usually ranges from 0.05 to 0.25, which gives the potential predicted wing lift curve slope in the range 0.0972 to 0.0975. The lift curve slope obtained from CFD was 0.0577 as shown in Figure 7.

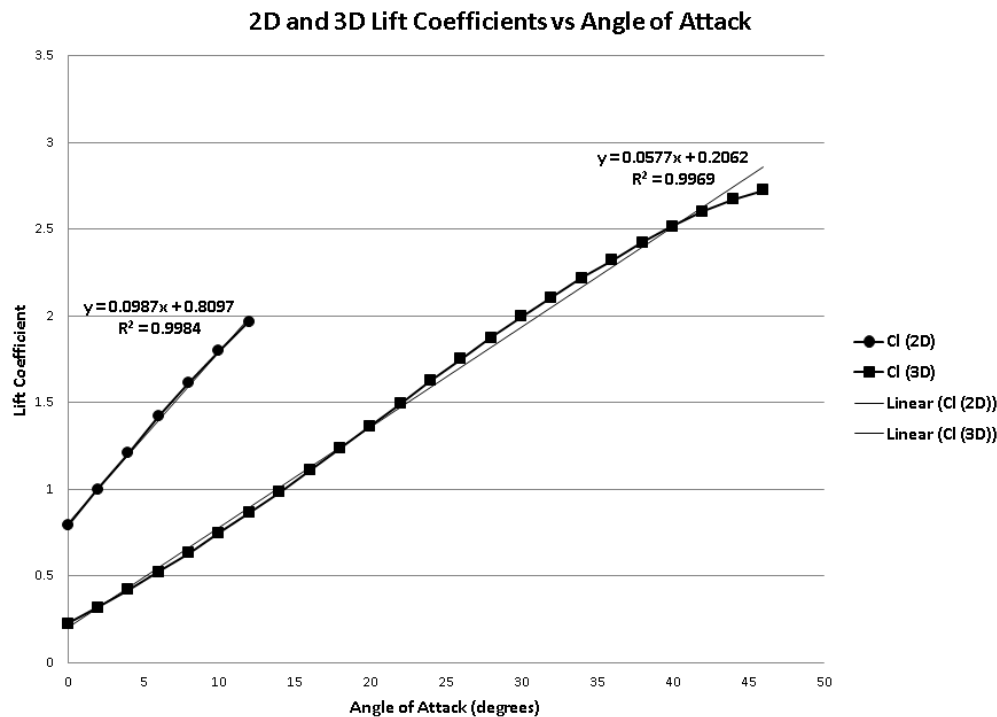


Figure 7: Comparison of 2D airfoil and 3D wingsuit lift coefficients vs. geometric angle of attack with linear curve fits

The discrepancy between the predicted slope a and that obtained by CFD can be partially explained by the phenomenon of the effective angle of attack. In fact, although the effective angle of attack given by Equation (3) assumes an elliptic wing and is therefore highly approximate, it demonstrates that the effective angle of attack is smaller than the geometric angle of attack. The effective angle of stall is thus between 27 and 32° rather than 48°. The induced angle of attack is large, and would be even larger if it could be calculated without the elliptic planform assumption. Plotting the 3D CFD results against the effective angle of attack rather than the geometric one brings the slope much closer to the expected value, with a value of 0.0964 as shown in Figure 8. Again, this result comes about from a big assumption and should

not be taken as numerically accurate, but the fact that the data shifts in the correct direction and comes closer to the expectation is reassuring.

2D and 3D Lift Coefficients vs Angle of Attack

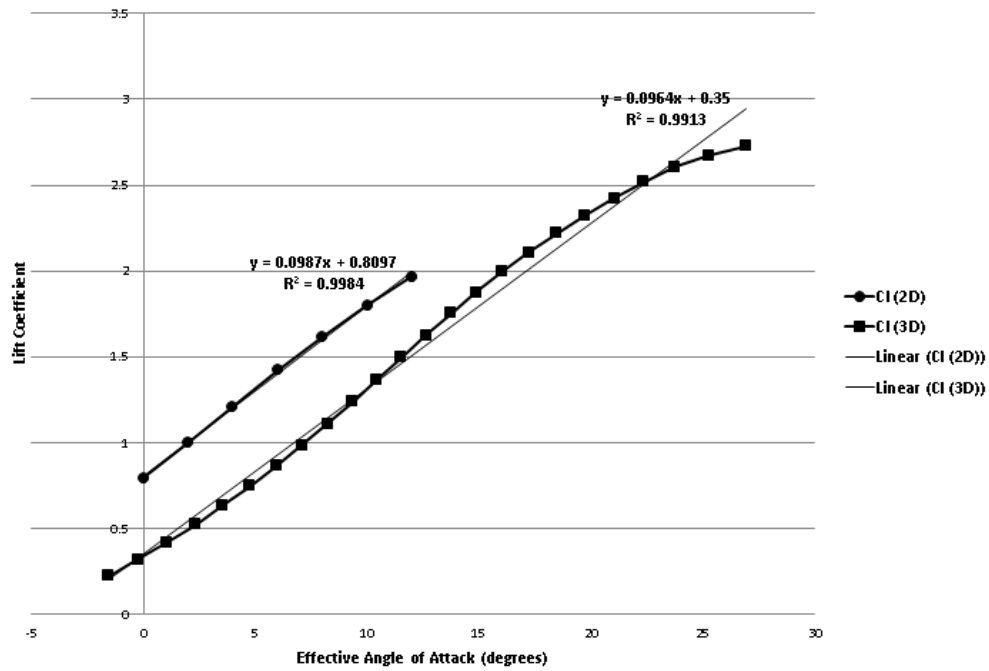


Figure 9: Comparison of 2D airfoil and 3D wingsuit lift coefficients vs. effective angle of attack with linear curve fits

Knowing more about the airflow as the angle of attack increases is useful in understanding how the wingsuit would behave in actual flight conditions. The 2D pressure plots for various cross sections of the wingsuit were generated with the sectional views as shown in Figure 9.

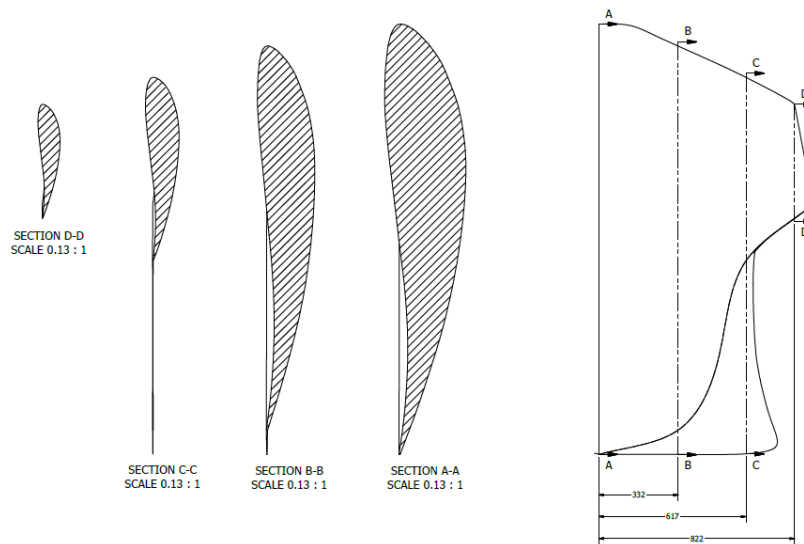


Figure 8: 2D cross sections and locations A through D at z = 0.000, 0.332, 0.617, and 0.822 m from center line of the wingsuit

The pressure plots are given in Figure 10. For each cross section, the pressure coefficient is plotted at 24, 32, 40, and 48° angles of attack. The plots show the expected trend in which the suction peak at the front of the airfoil increases with angle of attack until stall, at which point it

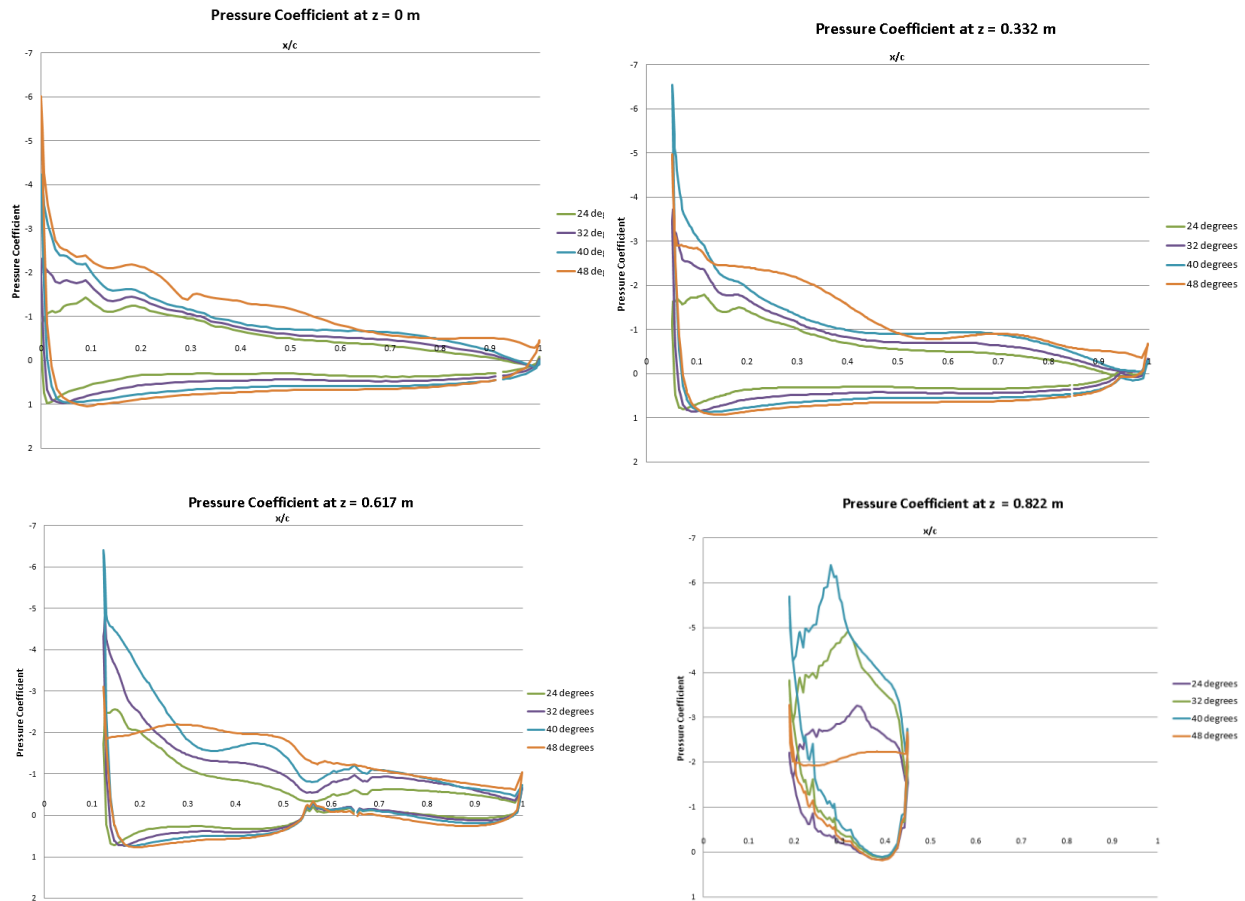


Figure 10: Pressure coefficient vs. x/c for 8, 16, 24, 32, 40, and 48° angles of attack at $z = 0.000$ m, 0.332 m, 0.617 m, and 0.822 m from centerline of the wingsuit begins to decrease.

Finally, the flow can also be visualized in 3D. Figure 11 shows the velocity streamlines colored by the turbulent eddy viscosity, which demonstrate the typical vortical motion near the edges of a wing. Figure 11 shows the wing tip vortices at 12° and 32° angle of attack; the motion from the wing tips increases in size and generated turbulence as the angle of attack increases. In Figure 12, the pressure contours on the wingsuit are visible as well as the velocity streamlines. The edges of the wing also show lower pressure zones, and there is higher pressure on the back side of the airfoil than on the front side.

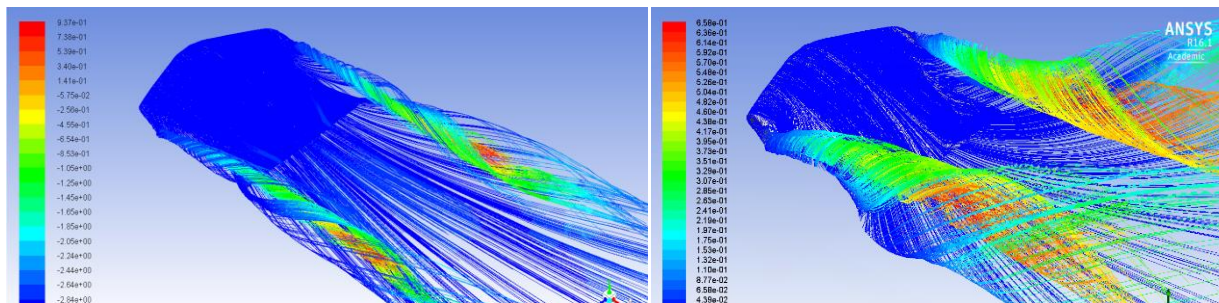


Figure 11: 3D wingsuit at 45 m/s and 12° (left) and 32° (right) angles of attack with streamlines colored by modified turbulent viscosity

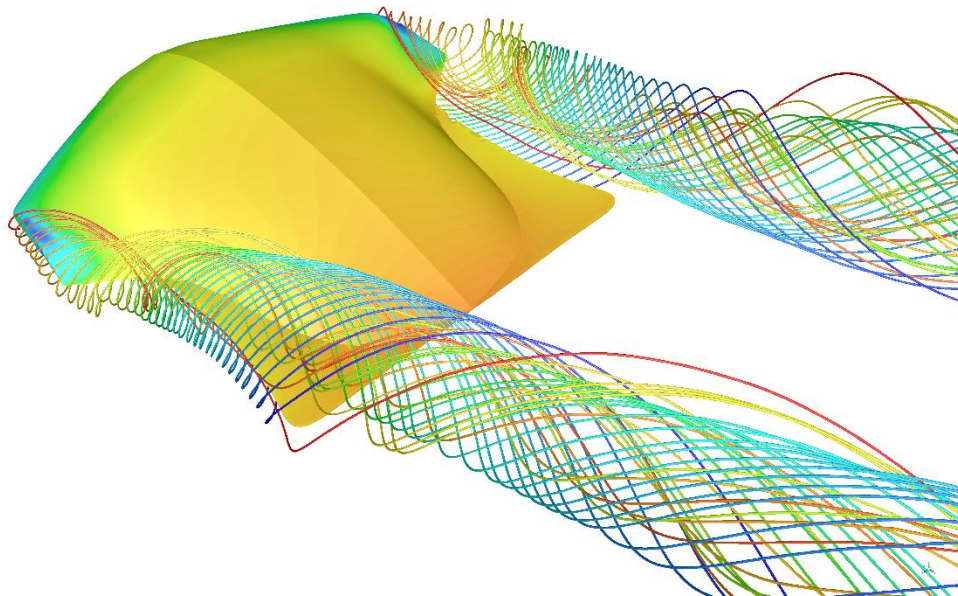


Figure 12: 3D wingsuit at 45 m/s and 32° angle of attack with surface pressure contours and velocity streamlines from wing edges

Conclusions and Future Work

One of the major problems in research related to wingsuits is the lack of information available in the literature; however each research project helps lay the groundwork for the next project and eventually they will result in a more solid foundation to build upon. This study turned the lack of information on wingsuit geometry into an opportunity to examine the behavior of an ideal wingsuit with an airfoil cross section. Future work might include more realistic geometries that take into account human features, and perhaps a flexible geometry that simulates the motion of the flexible wingsuit fabric. Using the pressure coefficient data and velocity streamlines, more details should be acquired regarding the changes in the behavior of the airflow about the wingsuit as the angle of attack is increased. Although the validation techniques for the 3D case seemed to indicate that the results of this simulation were reasonable, the values should be compared to experimental data if possible. It might also be worthwhile to run the same cases with different turbulence models to gain more confidence in the simulation results.

References

- [1] W. S. Weed, "The Flight of the Bird Men," 18 June 2003. [Online].
- [2] J. John D. Anderson, *Fundamentals of Aerodynamics*, New York, NY: McGraw Hill, 2011.
- [3] G. Robson and R. D'Andrea, "Longitudinal Stability Analysis of a Jet-Powered Wingsuit," *AIAA Guidance, Navigation, and Control Conference*, 2010.

Acknowledgements

I would like to extend my sincerest thanks to Dr. Ramesh Agarwal for his support of an unconventional topic and his guidance throughout the entire design and analysis process. I would also like to thank Dr. Qiulin Qu, whose input was invaluable to this project. Thanks to fellow CFD lab member Boshun Gao for his instructions and assistance with ANSYS software. Finally, an enormous thank to the NASA – Missouri Space Grant Consortium for the funding that made this project possible.

Biography

Maria Ferguson is a Master's of Aerospace Engineering candidate in the department of Mechanical Engineering and Materials Science at Washington University in St. Louis. She graduated with honors with a Bachelor of Arts from Saint Mary's College and a Bachelor of Science in Mechanical Engineering from Washington University in 2016 through the Dual Degree program. Hailing from Napa, California, she hopes to secure a position as an Aerodynamics Engineer in industry after graduation and one day fly her own wingsuit.